

# The iron abundance in four planetary nebulae

M. Perinotto<sup>1</sup>, C.G. Bencini<sup>1</sup>, A. Pasquali<sup>2</sup>, A. Manchado<sup>3</sup>, J.M. Rodriguez Espinosa<sup>3</sup>, and R. Stanga<sup>1</sup>

<sup>1</sup> Dipartimento di Astronomia e Scienza dello Spazio, Università di Firenze, L.go E. Fermi 5, I-50125 Firenze, Italy

<sup>2</sup> ST-ECF/ESO, Karl-Schwarzschild-Strasse 2, D-85748 Garching bei München, Germany

<sup>3</sup> Instituto de Astrofísica de Canarias, Spain

Received 22 December 1998 / Accepted 11 February 1999

**Abstract.** We have observed the high excitation planetary nebulae NGC 7027, NGC 6543 and the low excitation planetaries Hu 2-1 and Cn 3-1 in the optical & near IR with the aim to contribute accurate measurements of their gaseous iron abundances. Use was made of multi-level atomic models of iron ions to interpret the observed forbidden lines of various iron ions. The resulting total abundances are:  $N(\text{Fe})/N(\text{H})=(4 \pm 2) \times 10^{-7}$ ,  $(3 \pm 2) \times 10^{-6}$ ,  $(9 \pm 4) \times 10^{-7}$ ,  $(6 \pm 3) \times 10^{-7}$ , in NGC 7027, NGC 6543, Hu 2-1, Cn 3-1, respectively. They are believed to be more accurate than previous determinations for NGC 7027 & NGC 6543 (no previous data were available for the other two PNe). The corresponding depletion factors are 80, 11, 36 and 53, respectively. We don't see in this limited sample of PNe any indication that the depletion factors are linked with properties like the excitation of the nebula or its age.

**Key words:** ISM: planetary nebulae: general – ISM: planetary nebulae: individual: Cn 3-1; Hu 2-1; NGC 6543; NGC 7027

## 1. Introduction

The abundance of iron in planetary nebulae (PNe) has been scarcely studied so far essentially because of the relative faintness of its observed emission lines. After the first studies by Shields (1975; 1978) and Garstang et al. (1978), apparently only Clegg et al. (1987a; 1987b) and Middlemass (1990) have addressed the matter. Nevertheless the knowledge of the abundance of iron in PNe is quite important in various respects. One of these is to establish, via comparison with the corresponding abundances of the photospheres of their central stars, the effective iron grain production from the AGB to PNe phases.

A general result of these works is that the derived abundance of iron/hydrogen in PNe is quite less than in the Sun, being smaller by a factor between 5 and 100. This has been interpreted as an effect of depletion of gaseous iron into dust grains.

Although the chemical composition of grains associated with PNe gas is still essentially unknown, it is assumed that PNe grains should not differ substantially from those in the interstellar medium. Their composition is thus believed to consists

of carbon dominated material and/or silicates of various species (cf. Mathis, 1990). On the other hand the above large depletion factors suggest that iron might play some role in the composition of cosmic grains in particular PNe. There are then reasons that justify to put some effort to provide new determinations of the abundance of gaseous iron in PNe.

Previous determinations have been based on the use of few forbidden emission lines in the visual and near infrared wavelength regions, interpreted essentially with two-level model atoms. An adequate representation of the reality requires instead to take into account the inter-relationships among the numerous levels of the atomic structure of iron ions. This was not possible until recently, when mainly in connection with the Iron-Project (Hummer et al., 1993), precise values for the needed atomic quantities for up to hundred levels have been calculated. These results are clearly fundamental to obtain reliable abundances of iron ions. We are making use of them in the present study. In addition accurate flux measurements of the faint iron lines produced in PNe are also in order.

For this purpose, we have observed four PNe of different excitation class with the WHT 4.2m telescope at La Palma, covering the spectral range from the blue to the near IR.

Sect. 2 contains the observations and data reduction, Sect. 3 the method to derive the iron abundance. In Sect. 4 we present the obtained abundances. The discussion then follows in Sect. 5.

## 2. Observations and data reduction

We observed Cn 3-1, Hu 2-1, NGC 6543 and NGC 7027 with the spectrograph ISIS mounted on the WHT 4.2m telescope (La Palma), in June 22–24, 1992 in the spectral range from 3650 Å to 9650 Å.

We used the 600 gr/mm grating together with the dichroic in order to simultaneously acquire spectra on both the blue and red arms of the spectrograph. The ISIS blue arm was equipped with a TEK1 CCD  $1124 \times 1124$  pixels, while the red arm was coupled with a EEV3 CCD  $1280 \times 1180$  pixels. The journal of the observations, with the relevant spectral ranges, is reported in Table 1. The corresponding dispersions for each grating central wavelength  $\lambda_c$  set-up are reported in Table 2. A longslit (4 arcminutes  $\times$  1 arcsec) was employed for the observations.

**Table 1.** Journal of observations: grating 600.

Date July	PNe	$\lambda_c$ (in Å)	ISIS arm	Range (in Å)	Expos. (in sec)	
22-23	Cn 3-1	4050	B	3670÷4469	300	
		4950	B	4550÷5350	300	
		4950	B	4550÷5350	60	
		5545	B	5169÷5977	1800	
		5950	R	5550÷6350	1800	
		6700	R	6300÷7100	300	
		6700	R	6300÷7100	60	
		9160	R	8717÷9642	1200	
	Hu 2-1	4050	B	3670÷4469	900	
		4950	B	4550÷5350	120	
		4950	B	4550÷5350	30	
		9160	R	8717÷9642	1800	
	23-24	NGC 7027	4050	B	3670÷4469	600
			4050	B	3670÷4469	100
	22-23		4950	B	4550÷5350	30
			4950	B	4550÷5350	5
23-24		5545	B	5169÷5977	600	
		5550	R	5117÷6035	120	
22-23		5950	R	5550÷6350	600	
23-24		5950	R	5550÷6350	600	
		5950	R	5550÷6350	100	
22-23		6700	R	6300÷7100	30	
		6700	R	6300÷7100	15	
		6700	R	6300÷7100	240	
		9160	R	8717÷9642	300	
		9160	R	8717÷9642	60	
		9160	R	8717÷9642	1200	
23-24	NGC 6543	4050	B	3670÷4469	1200	
		4950	B	4550÷5350	120	
		4950	B	4550÷5350	30	
		4950	B	4550÷5350	120	
		5550	R	5117÷6030	1800	
		5550	R	5117÷6030	300	
		6700	R	6300÷7100	120	
		6700	R	6300÷7100	30	
		6700	R	6300÷7100	30	
		6700	R	6300÷7100	120	
		9160	R	8717÷9642	600	
		9160	R	8717÷9642	1200	

We acquired bias, flat-field frames and CuNe lamp comparison spectra for each grating  $\lambda_c$  set-up, while the standard stars BD262606 and BD174708 were observed for flux calibration.

Following the corrections for bias and flat-field and cosmic rays removal, the data were reduced by means of the IRAF/LONGSLIT package which allows for 2D- wavelength- and flux- calibration of the spectra. The net result of this calibration procedure is that every position along the spatial axis of the spectra is characterized in wavelength and flux.

In all spectra of Table 1 the individual emission lines have been measured and averaged out to produce a final list of the fluxes with their errors. The spectra of the same object in different wavelength ranges have been linked together using the lines in common. In some cases where there was not a sufficient wavelength overlap, we have dereddened the separate spectra

**Table 2.** Spectral dispersions.

Grating	$\lambda_c$ (in Å)	Dispersion (Å/pix)
600	4050	0.78
	4145	0.78
	4195	0.78
	4945	0.78
	5545	0.79
	5551	0.74
	5950	0.99
	6700	0.80
	9160	0.75

using the best values in the literature of the extinction at  $H\beta$ ,  $C_\beta$ , together with the extinction curve by Mathis (1990). We have then checked the observed Balmer decrement vs the theoretical one for case B nebulae (Hummer & Storey, 1987). In a few cases the observed individual hydrogen line intensities did disagree up to 30% with the theoretical ones across the separate spectra. To overcome these discrepancies we have normalized  $H\gamma/H\beta$  or  $H\delta/H\beta$ , depending on whether  $H\gamma$  or  $H\delta$ , respectively, was the best observed line, to the theoretical value.

The final intensities have been compared with determinations from other authors as follows: Keyes et al. (1990) for NGC 7027, and Aller & Czyzak (1979) for NGC 6543, Hu 2-1 and Cn 3-1. The agreement is better than 5% for the lines with observed flux  $F_{\text{obs}} > 10$  ( $H\beta = 100$ ), 10% if  $F_{\text{obs}} > 1$ , 30% if  $F_{\text{obs}} > 0.1$  and about 50% for  $F_{\text{obs}} > 0.01$ . We have adopted such values as percentage errors of our measured line fluxes.

For dereddening the entire spectra we have adopted  $C_\beta = 1.38$  for NGC 7027, 0.12 for NGC 6543 and Cn 3-1 and 0.34 for Hu 2-1 (Cahn et al., 1992)

We present in Table 3, 4, 5 and 6 the measured fluxes of iron lines in NGC 7027, NGC 6543, Cn 3-1 and Hu 2-1, respectively. We also report iron lines which are possibly blended with lines of other ions. These lines, however, have not been used in the subsequent analysis.

### 3. Method of analysis of line intensities

We have identified in our objects some iron permitted lines: 2 of FeI, 4 of FeII, and 1 of FeIII and a number of forbidden lines. In addition to blended lines, we have disregarded lines with observed fluxes fainter than 0.05 in the usual  $H\beta = 100$  scale. As with permitted Fe lines, we are thus restricted to FeI  $\lambda$  3920.3,  $\lambda$  6393.6 and FeII  $\lambda$  5197.6,  $\lambda$  6516.1. We have not derived ionic abundances from these lines because we are not aware of effective recombination coefficients for these lines.

We have identified forbidden lines of FeII, FeIII, FeV, FeVI and FeVII. The best way to derive ionic abundances from these lines is to use a complete set of statistical equilibrium equations for all relevant levels, considering the physical properties of the specific nebulae. Because of the atomic structure of the iron ions, and the electron temperature prevailing in the various ionizations zones of the nebulae, the number of levels to be taken into account is rather high.

**Table 3.** Iron emission lines in NGC 7027.  $F(H\beta)$  is  $8.99 \times 10^{-12}$  erg cm $^{-2}$ . Both the observed and the dereddened fluxes ( $C_\beta=1.38$ ) are in the scale of  $F(H\beta)=100$ . The symbol “:” denotes an uncertainty of 50%.

$\lambda$ (Å)	Ion	Flux obs.	Flux der.
3774.0	OIII+[FeVI]	0.10	0.23
3895.7	[FeV]	0.03:	0.07:
4129.3	OII+[FeIII]	0.03:	0.05:
4181.3	[FeV]	0.02:	0.04:
4287.4	[FeII]	0.15	0.24
4658.1	[FeIII]+CIV	0.56	0.65
5146.8	[FeVI]	0.17	0.14
5158.8	[FeII]	0.11	0.09
5177.0	[FeVI]	0.14	0.11
5197.6	FeII	0.34	0.26
5199.2	[FeII]	0.17	0.13
5254.9	FeII+CrI	0.02:	0.02:
5261.6	[FeII]	0.04:	0.03:
5270.4	[FeIII]	0.09	0.07
5276.1	[FeVII]+FeII	0.10	0.07
5336.4	[FeVI]+CII	0.13	0.09
5425.3	[FeVI]	0.11	0.07
5485.7	[FeVI]	0.06	0.04
5556.3	[FeII]	0.05	0.03
5631.6	[FeVI]	0.11	0.06
5678.0	[FeVI]	0.14	0.08
5720.9	[FeVII]	0.33	0.18
5867.2	[FeI]	0.25	0.13
6393.6	FeI	0.08	0.03
6516.1	FeII	0.08	0.03
6599.7	[FeVII]	0.17	0.06

**Table 4.** Iron emission lines in NGC 6543.  $F(H\beta)$  is  $1.22 \times 10^{-11}$  erg cm $^{-2}$ . Both the observed and the dereddened fluxes ( $C_\beta=0.12$ ) are in the scale of  $F(H\beta)=100$ . The symbol “:” denotes an uncertainty of 50%.

$\lambda$ (Å)	Ion	Flux obs.	Flux der.
3762.9	FeII+NIII	0.27	0.30
3964.6	FeII+HeI	0.77	0.82
4319.6	[FeII]	0.13	0.13
4416.3	[FeII]	0.08	0.08
4604.5	[FeII]	0.04:	0.04:
4607.0	[FeIII]	0.10	0.10
4658.1	[FeIII]	0.23	0.24
4924.5	[FeIII]+OII	0.09	0.09
5197.6	FeII	0.05	0.05
5199.2	[FeII]	0.03:	0.03:
5270.4	[FeIII]	0.10	0.10
5336.4	[FeVI]	0.02:	0.02:
5525.1	FeII	0.02:	0.02:
5529.9	FeII	0.03:	0.03:
5615.7	FeI+[CaVII]	0.01:	0.01:
5929.5	FeIII	0.02:	0.02:

**Table 5.** Iron emission lines in Cn 3-1.  $F(H\beta)$  is  $2.86 \times 10^{-12}$  erg cm $^{-2}$ . Both the observed and the dereddened fluxes ( $C_\beta=0.12$ ) are in the scale of  $F(H\beta)=100$ .

$\lambda$ (Å)	Ion	Flux obs.	Flux der.
3964.6	FeII+HeI	0.93	0.99
4658.1	[FeIII]	0.31	0.31
4881.0	[FeIII]	0.19	0.19
5158.3	[FeII]	0.14	0.13
5197.6	FeII	0.15	0.15
5199.2	[FeII]	0.08	0.08
5270.4	[FeIII]	0.31	0.30

**Table 6.** Iron emission lines in Hu 2-1.  $F(H\beta)$  is  $4.92 \times 10^{-12}$  erg cm $^{-2}$ . Both the observed and the dereddened fluxes ( $C_\beta=0.34$ ) are in the scale of  $F(H\beta)=100$ .

$\lambda$ (Å)	Ion	Flux obs.	Flux der.
3920.3	FeI	0.12	0.15
3964.6	FeII+HeI	0.86	1.03
4416.3	[FeII]	0.10	0.11
4658.1	[FeIII]	0.39	0.40
4701.5	[FeIII]	0.13	0.13
4881.0	[FeIII]	0.20	0.20
5270.4	[FeIII]	0.24	0.22

One basic difficulty which prevented so far from applying this procedure has been the lack of the needed atomic quantities, i.e. the collision strengths by electron impact and the radiative transition probabilities, for all pairs of atomic levels. Consequently, almost all the determinations of iron abundances in PNe have been based on the assumption of two levels approximation in the evaluation of the population of upper levels of the observed transitions.

Recent extensive calculations of atomic quantities allow now to use the complete set of statistical equilibrium equations for a substantial number of levels.

The chemical abundance of a specific iron ion comes then from each observed line intensity  $F(ji)$  between upper level  $j$  and lower level  $i$  from the equation:

$$\frac{N_1(Fe^{+x})}{N(H^+)} = \frac{F_{ji}}{F_{H\beta}} \frac{N_1(Fe^{+x})}{N_j(Fe^{+x})} \frac{N_e \alpha_\beta^{eff} h\nu_\beta}{A_{ji} h\nu_{ij}} \quad (1)$$

where  $A_{ji}$  is the radiative transition probability,  $h\nu_{ij}$  the energy difference between the levels,  $\alpha_\beta^{eff}$  is the effective recombination coefficient of  $H\beta$ ,  $N_e$  the electron density (cm $^{-3}$ ),  $N_j(Fe^{+x})$  and  $N_1(Fe^{+x})$  the population of level  $j$  and of the ground level of  $Fe^{+x}$ , respectively.

The ratio  $N_j/N_1$  depends significantly on the electron temperature, which must then be evaluated with care. Therefore, we need to obtain mean temperatures representative of the nebular zones where the various iron ions are dominant.

**Table 7.** Nebular radius in parsec; distances in kpc. The iron abundances of the 4 PN, of sulphur and chlorine for Hu 2-1 and of chlorine for NGC 7027 are the solar ones. Otherwise chemical abundances are from Aller & Czyzak (1983) for Cn 3-1 and NGC 6543; Beintema et al. (1996) for NGC 7027; Henry et al. (1996) for Hu 2-1, except for argon from French (1981).

PN	Cn 3-1	Hu 2-1	NGC 6543	NGC 7027
Dist.	2.7	3.1	1.4	0.8
$T_*$	31000	35000	60000	161000
$L/L_\odot$	$3.7 \times 10^3$	$1.2 \times 10^4$	$5.6 \times 10^3$	$6.9 \times 10^3$
$R/R_\odot$	2.57	3.01	0.702	0.109
$N_e$	$4.0 \times 10^3$	$1.7 \times 10^4$	$3.6 \times 10^3$	$2 \times 10^4$
$r_{\text{neb}}$	0.052	0.020	0.070	0.027
He/H	0.13	0.11	0.112	0.10
C/H	$5.0 \times 10^{-4}$	$5.6 \times 10^{-4}$	$1.3 \times 10^{-3}$	$7.4 \times 10^{-4}$
N/H	$4.9 \times 10^{-5}$	$1.2 \times 10^{-4}$	$8.7 \times 10^{-5}$	$1.3 \times 10^{-4}$
O/H	$1.3 \times 10^{-4}$	$3.1 \times 10^{-4}$	$5.6 \times 10^{-4}$	$4.5 \times 10^{-4}$
Ne/H	$8.5 \times 10^{-5}$	$3.4 \times 10^{-5}$	$1.4 \times 10^{-4}$	$6.2 \times 10^{-5}$
S/H	$2.5 \times 10^{-6}$	$1.6 \times 10^{-5}$	$1.0 \times 10^{-5}$	$5.6 \times 10^{-6}$
Cl/H	$1.3 \times 10^{-7}$	$2.0 \times 10^{-7}$	$3.0 \times 10^{-7}$	$2.0 \times 10^{-7}$
Ar/H	$1.5 \times 10^{-6}$	$7.9 \times 10^{-7}$	$2.6 \times 10^{-6}$	$2.2 \times 10^{-6}$
Fe/H	$3.2 \times 10^{-5}$	$3.2 \times 10^{-5}$	$3.2 \times 10^{-5}$	$3.2 \times 10^{-5}$

This can be done making use of detailed photoionization models for the individual nebulae which also allow to estimate the contribution of unseen ions to the total iron abundance.

### 3.1. Atomic models

In evaluating the number of levels to be considered for the various iron ions, we have noted that in high excitation PNe, ions with the highest ionization potential observed (usually NeV) emit lines starting at most from levels excited about 8 eV above the ground level. In the external ionized regions of PNe, the observed lines of ions like NII come from levels excited about 4 eV.

It is then reasonable to consider atomic models spanning from levels excited about 8–9 eV (in case of FeVII) down to 4 eV (for FeII).

We have found in the literature that the needed atomic quantities have been calculated in the ions FeVII, FeVI, FeV, FeIII, FeII for 9, 19, 5, 25, 35 levels, respectively. The above correspond to energies of the most excited levels of 8.3, 8.9, 0.2, 5.3 and 3.9 eV, respectively. The available data are then adequate for all the above ions except FeV, for which however we don't have well measured lines.

For the various ions the following atomic data have been used: FeVII, A(j,i) (Nussbaumer & Storey, 1982),  $\Omega_{ij}$  (Keenan & Norrington, 1987); FeVI, A(ji) and  $\Omega_{ij}$  (Nussbaumer & Storey, 1978). In the case of FeIII we have used two sets of transition probabilities: i) from Quinet (1996), ii) from Nahar & Pradhan (1996), and the  $\Omega_{ij}$  by Zhang (1996). For FeII we also have used two sets of transition probabilities: i) from Quinet et al. (1996), ii) in part from Garstang (1962) and in part from

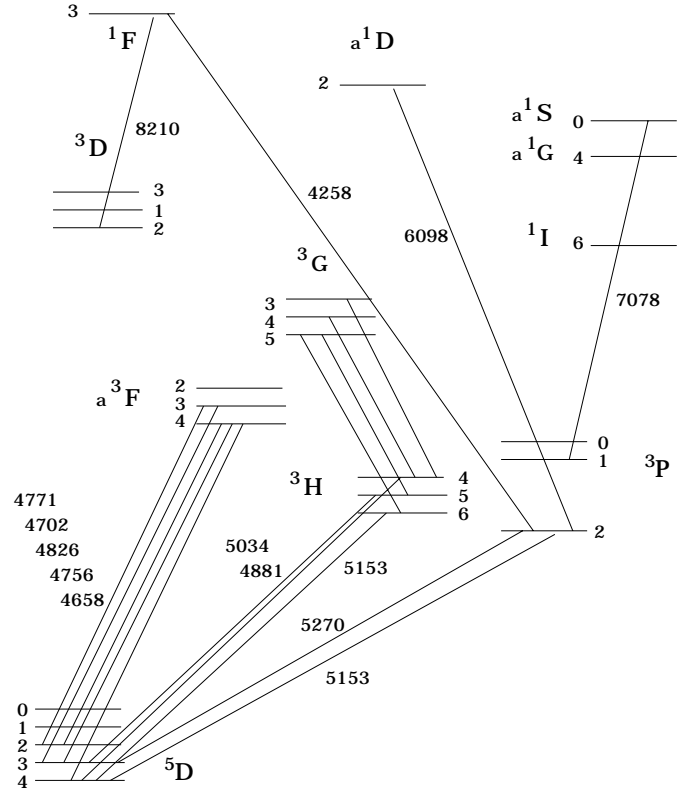


**Fig. 1.** Grotrian diagram of FeIII.

Nussbaumer & Storey (1988). The  $\Omega_{ij}$  of FeII are from Zhang & Pradhan (1995).

As an illustration of the atomic models, we present in Fig. 1 the levels used for FeIII.

### 4. Derived iron abundance

We have used the most recent version of the CLOUDY photoionization code (version 90.04 updated to October, 21, 1997; cf. Ferland, 1996) assuming spherical symmetry and constant electron density. For each PN we have calculated specific models based on the best knowledge of the relevant parameters which are reported in Table 7. And in addition models corresponding to a distance a factor 1.5 larger or smaller than the “adopted” distance. This was done by correspondingly modifying the stellar radius and consequently the stellar luminosity. Moreover we have calculated models with parameters corresponding to the adopted distance, but with a stellar temperature higher or lower than the adopted  $T_{\text{eff}}$  by 20% in the high excitation nebulae NGC 7027 and NGC 6543, and by 10% in the low excitation ones, Hu 2-1 and Cn 3-1. It can be proved in fact that a 20% error, while possible in the two excited nebulae, is certainly too large in our low excitation PNe.

These various models have allowed us to have an estimate of the uncertainties in the quantities we derive from the photoionizations models: (i) the behaviour of the electron temperature and (ii) the iron ionization structure.

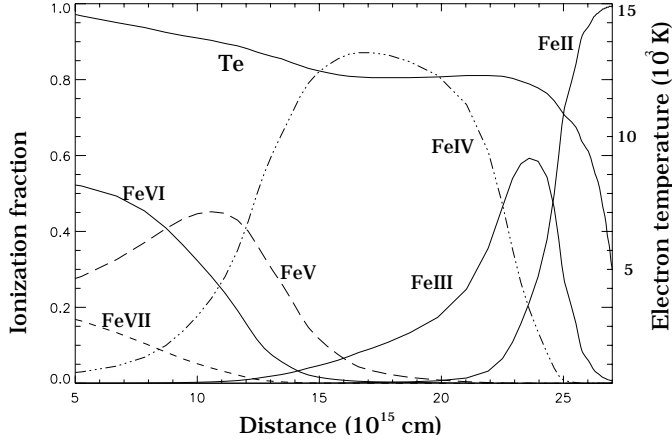


Fig. 2. Iron ionization structure and Te behaviour in NGC 7027.

#### 4.1. NGC 7027

It is one of the most excited PNe, with a morphology not properly spherical and a mean optical diameter of  $14''$ . Its central star is very faint ( $V=16.25$ ) (cf. Acker et al. 1992). The distance can be assumed to be 0.8 kpc (Acker et al. 1992; Middlemass, 1990) with an uncertainty up to  $\sim 50\%$  considering the dispersion of the existing determinations. The external nebular radius is consequently 0.027 pc. According to the recent paper by Beintema et al. (1996), the central star has  $T_{\text{eff}}$  equal to 161,000 K and  $L/L_{\odot} = 6900$  K, while the nebular electron density is  $2 \times 10^4 \text{ cm}^{-3}$ . We have used these quantities as input parameters for CLOUDY. They are listed in Table 7 together with analogous quantities assumed for the other PNe of our sample.

The input iron abundance for CLOUDY has been set to solar for all four PNe. A different choice has no influence into the quantities we are interested in: temperature behaviour and iron ionization structure. With the entries of Table 7, the photoionization model of NGC 7027 results to have a nebular size too small when compared to the observed one. Since the electron density plays a role in this respect, we have lowered it to  $7 \times 10^3 \text{ cm}^{-3}$ . With this density the nebula becomes optically thick at a radius of 0.028 pc, quite close to the observed one.

The resulting ionization structure of iron is shown in Fig 2 together with the radial distribution of the electron temperature. The corresponding ionic fractional abundances, averaged on the volume of NGC 7027, are 0.125 for FeII, 0.126 for FeIII, 0.362 for FeIV, 0.165 for FeV, 0.174 for FeVI and 0.047 for FeVII. We have also evaluated average volume weighted temperatures for the single iron ions for subsequent use in the calculation of the statistical equilibrium:

$$T_e(\text{Fe}^{+i}) = \frac{\int N(\text{Fe}^{+i})T_e 4\pi r^2 dr}{\int N(\text{Fe}^{+i})4\pi r^2 dr}. \quad (2)$$

The obtained temperatures are 9114 K, 11700 K, 12230 K, 13250 K, 13770 K and 14050 K for FeII, FeIII, FeV, FeVI and FeVII respectively. We have then applied Eq. 1 to derive the ionic abundance for each observed forbidden line. The results are given in Table 8.

**Table 8.** Abundances of iron ions in NGC 7027. The flux is dereddened and normalized to  $H\beta = 100$ . <sup>a</sup> indicates the ionic abundances derived from the  $A_{ji}$  values of Quinet et al. (1996). <sup>b</sup> and <sup>c</sup> mark the ionic abundances calculated with the  $A_{ji}$  values given by Nussbaumer & Storey (1988) and Garstang (1962) and Nahar & Pradhan (1996), respectively.

ion	$\lambda$	flux	$N(\text{Fe}^{+i})/N(\text{H}^+)$		
[FeII]	5158.8	0.09	$1.7 \times 10^{-6a}$		
			$2.2 \times 10^{-6b}$		
[FeIII]	4658.1	0.65	$1.1 \times 10^{-7a}$		
			$2.9 \times 10^{-7c}$		
[FeVI]	5270.4	0.07	$4.2 \times 10^{-8a}$		
			$4.6 \times 10^{-8c}$		
			3774.0	0.23	$6.0 \times 10^{-5}$
			5146.8	0.14	$6.4 \times 10^{-8}$
[FeVII]	5177.0	0.11	$7.3 \times 10^{-8}$		
			5336.4	0.09	$6.1 \times 10^{-8}$
			5425.3	0.07	$9.3 \times 10^{-8}$
			5631.6	0.06	$7.5 \times 10^{-8}$
[FeVII]	5678.0	0.08	$1.1 \times 10^{-7}$		
			5276.1	0.07	$4.3 \times 10^{-7}$
	5720.9	0.19	$8.1 \times 10^{-8}$		

In the case of FeII two sets of atomic data are available with rather different  $A_{ji}$  values in some transitions (cf. Sec. 3.1). We have employed both sets to calculate the FeII abundance. The results are listed in column 4 of Table 8, the first and the second rows corresponding to Quinet et al.'s (1996)  $A_{ji}$  and to those from Nussbaumer and Storey's (1988) - Garstang's (1962), respectively. A similar situation holds for FeIII:  $A_{ji}$  values have been calculated by Quinet et al. (1996) and by Nahar & Pradhan (1996). The corresponding ionic abundances are listed in the first and second rows of the Table, respectively, for each of the two [FeIII] lines. The two pairs of atomic data sets did provide the same ionic abundances to within a 30% uncertainty at most, except in the case of the [FeIII]  $\lambda 4658.1$  line, where they disagree by a factor of 3.

We have then averaged the derived abundances of FeII by weighting twice the abundances calculated from Quinet et al.'s (1996) data, since their atomic data are more complete. It turns out that the FeII abundance is quite high with respect to that of the other ions listed in Table 8. We believe that this may be due to a fluorescence effect. Fluorescence has indeed been invoked in order to reproduce the observed [FeII] line intensities in the Orion Nebula and other HII regions (Lucy, 1995). For this reason, we have not included the chemical abundances from [FeII] lines in the subsequent analysis.

A discrepancy is also seen between the [FeIII] lines in Table 8: the abundances from [FeIII]  $\lambda 4658.1$  and [FeIII]  $\lambda 5270.4$  differ by a factor 4. The higher abundance from [FeIII]  $\lambda 4658.1$  may be due to flux contamination, since this line is blended with a CIV emission at nearly the same wavelength. Consequently, we do not take it into account and rely on the abundance determined from [FeIII]  $\lambda 5270.4$ .

In the case of FeVI, the ionic abundances computed from the various observed lines are relatively close. Except for the line at  $\lambda 3774 \text{ \AA}$  which is a blend, the average from the other lines, using weights proportional to the line intensities, gives  $N(\text{Fe}^{+5})/N(\text{H}) = 7.7 \times 10^{-8}$ .

The FeVII abundances given by the two available lines differ by a factor 5 and appear also to be rather larger than expected from the ionization structure of NGC 7027. We have then decided not to include the results obtained for this ion.

In conclusion, the total abundance of iron has been determined using only the [FeIII] and [FeVI] lines and correcting for the other ions through the model ionization structure. The final value of the iron abundance is  $N(\text{Fe})/N(\text{H}) = 4.0 \times 10^{-7}$ . It refers to the stellar and nebular parameters adopted for NGC 7027 in Table 7. As we have already illustrated, we would like to allow for uncertainties in the distance and in  $T_{\text{eff}}$  of the central star. In order to quantify how these uncertainties hamper the abundance calculations, we have repeated the whole procedure for distances 1.5 larger and 1.5 smaller than 0.8 kpc (modifying accordingly the related parameters) and for a  $T_{\text{eff}}$  20% larger and smaller than 161,000 K. All these models have produced ionization structures consistent with the FeIII and FeVI abundances previously derived, except for the model with the smallest  $T_{\text{eff}}$  (130,000 K) which produces an extremely low [FeVI] ionization fraction. From all that we can estimate that the uncertainties in the derived total abundance of iron are of the order of 25%. However, since the faintest iron lines observed are accurate to about 50%, and considering that we have to disregard some ions for the reasons given above, while on the other hand the abundances of FeVI from different lines are quite close to each other, we consider reasonable to assign a 50% error to the total derived iron abundance in NGC 7027:

$$N(\text{Fe})/N(\text{H}) = (4 \pm 2) \times 10^{-7}.$$

This value is not too far from previous determinations:  $7 \times 10^{-7}$  and  $1 \times 10^{-6}$  by Shields (1975 and 1978, respectively) and  $1 \times 10^{-6}$  by Middlemass (1990). Considering the method we have adopted, we believe that our determination and its error are based on more realistic grounds.

#### 4.2. NGC 6543

It is a medium ionized nebula, with a complex main structure of about  $20''$  in diameter (Acker et al., 1992) and a faint extended halo (cf. Middlemass et al., 1989). For its distance we assume the average of the determinations reported by Acker et al. (1992) equal to 1.44 kpc.

The radius of the bright shell is then 0.070 pc, while its density is  $\log N_e = 3.60$  (Beintema et al. 1996). Using the parameters listed in Table 7 as inputs for CLOUDY, we have derived an iron ionization structure which gives the following fractional abundances, averaged on the volume: 0.103 for FeII, 0.196 for FeIII, 0.693 for FeIV and 0.007 for FeV. The corresponding temperatures, obtained as in NGC 7027, are: 7707 K, 8764 K, 8324 K and 8591 K respectively. The abundances of FeII and FeIII are given in Table 9. As in the case of NGC 7027, we have

**Table 9.** Abundances of iron ions in NGC 6543. The flux is dereddened and normalized to  $H\beta = 100$ . <sup>a</sup> indicates the ionic abundances derived from the  $A_{ji}$  values of Quinet et al. (1996). <sup>b</sup> and <sup>c</sup> mark the ionic abundances calculated with the  $A_{ji}$  values given by Nussbaumer & Storey (1988) and Gargstang (1962) and Nahar & Pradhan (1996), respectively.

ion	$\lambda$	flux	$N(\text{Fe}^{+i})/N(\text{H}^+)$
[FeII]	4319.6	0.13	$1.5 \times 10^{-6a}$ $2.4 \times 10^{-6b}$
	4416.3	0.08	$5.5 \times 10^{-7a}$ $4.8 \times 10^{-7b}$
[FeIII]	4607.0	0.10	$1.4 \times 10^{-6a}$ $1.9 \times 10^{-6c}$
	4658.1	0.24	$1.1 \times 10^{-7a}$ $2.8 \times 10^{-7c}$
	5270.4	0.07	$1.4 \times 10^{-7a}$ $1.6 \times 10^{-7c}$

neglected the FeII abundances because of possible fluorescence effects.

By averaging the [FeIII] abundances we have obtained  $N(\text{FeIII})/N(\text{H}^+) = 5.5 \times 10^{-7}$  and by correcting for the other ions through the ionization structure, a total iron abundance of  $N(\text{Fe})/N(\text{H}) = 2.8 \times 10^{-6}$ .

Also in this case, we have repeated the procedure changing the distance by a factor 1.5 relative to the adopted one and assuming  $T_{\text{eff}} = 48000 \text{ K}$  and  $72000 \text{ K}$ , respectively. We have finally derived a total iron abundance in NGC 6543:

$$N(\text{Fe})/N(\text{H}) = (3 \pm 2) \times 10^{-6}.$$

This disagrees significantly with the upper limit of  $3 \times 10^{-7}$  given by Paw et al. (1984) based on an entirely different technique, the lack of FeII absorption lines. We believe that our determination is more reliable.

#### 4.3. Hu 2-1

It is a low excitation compact nebula (Gurzadyan, 1997), with an angular size of  $2.6''$  (Acker et al., 1992). Its distance is estimated to be 3.1 kpc (Acker et al., 1992) and the electron density  $10^4 \text{ cm}^{-3}$  (Barker, 1978). The central star has a  $T_{\text{eff}}$  of 35,000 K (cf. Miranda, 1995) and a luminosity  $L/L_{\odot}$  of  $1.2 \times 10^4$  (Kaler & Jacoby, 1991; Zhang & Kwok, 1993). The linear size of the external radius is 0.02 pc. The adopted parameters are as usual reported in Table 7.

The fractional ionization abundances are: 0.049 for [FeII], 0.387 for [FeIII] and 0.564 for [FeIV] with related  $T_e$  of 8191 K, 9082 K and 9368 K, respectively. The calculated abundances of FeII and FeIII are reported in Table 10.

Since fluorescence may influence the [FeII] emission, we have not included as above this ion in the final calculation of the total iron abundance in Hu 2-1. We have also neglected the abundance derived from the [FeIII]  $\lambda 4881 \text{ \AA}$  line because it is three times larger than those computed from the other lines.

**Table 10.** Abundances of iron ions in Hu 2-1. The flux is dereddened and normalized to  $H\beta = 100$ . <sup>a</sup> indicates the ionic abundances derived from the  $A_{ji}$  values of Quinet et al. (1996). <sup>b</sup> and <sup>c</sup> mark the ionic abundances calculated with the  $A_{ji}$  values given by Nussbaumer & Storey (1988) and Gargstang (1962) and Nahar & Pradhan (1996), respectively.

ion	$\lambda$	flux	$N(\text{Fe}^{+i})/N(\text{H}^+)$
[FeII]	4416.3	0.11	$4.1 \times 10^{-7a}$ $3.5 \times 10^{-7b}$
[FeIII]	4658.1	0.40	$1.7 \times 10^{-7a}$ $4.2 \times 10^{-7c}$
	4701.5	0.13	$2.6 \times 10^{-7a}$ $3.7 \times 10^{-7c}$
	4881.0	0.20	$1.3 \times 10^{-6a}$ $1.1 \times 10^{-6c}$
	5270.4	0.22	$2.9 \times 10^{-7a}$ $3.3 \times 10^{-7c}$

The average of the remaining [FeIII] lines defines a total iron abundance of  $8.5 \times 10^{-7}$ .

With the procedure above described to estimate the uncertainties due to inaccuracies in the distance, and allowing for changes in  $T_{\text{eff}}$  by 10% in this low excitation object, we have obtained the final iron abundance of Hu 2-1:

$$N(\text{Fe})/N(\text{H}) = (9 \pm 4) \times 10^{-7}$$

This is the only Fe abundance determination available for Hu 2-1 so far.

#### 4.4. Cn 3-1

The nebula is of very low excitation, compact and slightly elliptical, with a mean diameter of  $8''$ . Aller & Czyzak (1983) and Kingsburgh & English (1992) measured an electron density of  $4 \times 10^3 \text{ cm}^{-3}$ . Miranda et al. (1997) have estimated a distance of 2.7 kpc, so that the external radius turns out to be 0.052 pc. The central star was found to have a  $T_{\text{eff}}$  of 31,100 K (Kaler & Jacoby 1991). From the evolutionary tracks by Blocker (1995) corresponding to a mass of  $0.6M_{\odot}$ , we have derived  $\log L/L_{\odot} = 3.73$ .

Given the above parameters, the CLOUDY fractional iron abundances are: 0.083 for FeII, 0.769 for FeIII and 0.148 for FeIV and the electron temperatures: 7608 K, 8336 K and 9193 K, respectively. The resulting abundances of FeII and FeIII are listed in Table 11.

As for Hu 2-1, we have disregarded the FeII abundances and neglected the abundance derived from the [FeIII]  $\lambda 4881 \text{ \AA}$  line.

$N(\text{FeIII})/N(\text{H})$  is then  $5.1 \times 10^{-7}$ . By correcting for the ionization structure we get  $N(\text{Fe})/N(\text{H}) = 6.7 \times 10^{-7}$ , and following the above procedure for estimating uncertainties on the derived abundances, we obtain a final iron abundance of:

$$N(\text{Fe})/N(\text{H}) = (6 \pm 3) \times 10^{-7}.$$

Also for this PN we are not aware of previous determinations of iron abundance.

**Table 11.** Abundances of iron ions in Cn 3-1. The flux is dereddened and normalized to  $H\beta = 100$ . <sup>a</sup> indicates the ionic abundances derived from the  $A_{ji}$  values of Quinet et al. (1996). <sup>b</sup> and <sup>c</sup> mark the ionic abundances calculated with the  $A_{ji}$  values given by Nussbaumer & Storey (1988) and Gargstang (1962) and Nahar & Pradhan (1996), respectively.

ion	$\lambda$	flux	$N(\text{Fe}^{+i})/N(\text{H}^+)$
[FeII]	5158.1	0.13	$3.5 \times 10^{-7a}$ $3.2 \times 10^{-7b}$
[FeIII]	4658.1	0.40	$1.8 \times 10^{-7a}$ $4.4 \times 10^{-7c}$
	4881.0	0.20	$1.9 \times 10^{-6a}$ $1.8 \times 10^{-6c}$
	5270.4	0.22	$5.1 \times 10^{-7a}$ $5.8 \times 10^{-7c}$

## 5. Discussion

We have obtained the following abundances of gaseous iron:  $N(\text{Fe})/N(\text{H}) = (4 \pm 2) \times 10^{-7}$ ,  $(3 \pm 2) \times 10^{-6}$ ,  $(9 \pm 4) \times 10^{-7}$ ,  $(6 \pm 3) \times 10^{-7}$ , in NGC 7027, NGC 6543, Hu 2-1, Cn 3-1, respectively. For the solar abundance we adopt  $3.2 \times 10^{-5}$  (Anders & Grevesse, 1989). This value comes from meteoritic studies, as it is now customary to give meteoritic values for solar abundances in the heaviest elements and the photospheric ones for C, N, O (cf. Savage & Sembach, 1966). It has been in fact shown (cf. Grevesse & Noels, 1993) that meteoritic and photospheric abundances agree to within 0.04 dex, resolving long standing discrepancies occurring for elements just like Fe. By comparison with the solar values we then find depletion factors of 80, 11, 36, 53, for NGC 7027, NGC 6543, Hu 2-1, Cn 3-1, respectively. Considering the uncertainties of our measurements of the iron abundances, only the value of NGC 6543 would result significantly different from those of NGC 7027 and Cn 3-1.

We don't see in this limited sample of PNe any suggestion that the depletion may be related with properties like the excitation of the nebula or its age, Hu 2-1 and Cn 3-1 being likely younger than the other two, owing to the smaller temperatures of their central stars, on the assumption of a similar mass for the four central star. An assumption however probably not in order for NGC 7027, which is considered to be more massive than average PNe.

Also we don't see a correlation with the chemical composition of the abundant heavy elements. All four PNe are in fact carbon rich objects with C/O equal to 1.6, 2.3, 3.8 and 1.8 in NGC 7027, NGC 6543, Hu 2-1 and Cn 3-1, while they have N/O equal to 0.29, 0.16, 0.38, 0.39, respectively (see Table 7). For comparison the Sun has 0.56 and 0.12 for the two ratios.

It is instead worth noticing that NGC 7027 has the highest reddening:  $C_{\beta} = 1.38$  as compared with 0.12, 0.34 and 0.12 for NGC 6543, Hu 2-1 and Cn 3-1 (see Sect. 2).

A significant part of the reddening in NGC 7027 has been found to be of local nebular origin (Perinotto et al., 1980), while we don't have any information about the local reddening in the other three PNe. Considering however their lower reddening

and larger distances relative to NGC 7027, we may infer no significant reddening by the nebular local dust in them. One might argue on whether this effect might be linked to a higher density in NGC 7027, but the four PNe do have all a relative high Ne. On the other hand NGC 7027 might have a more massive nebula, as above recalled, and therefore it is neither clear whether its dust-to-gas ratio is higher. This possibility would be of interest of course in connection with the search for an explanation of the highest iron depletion seen in NGC 7027 as it would suggest that higher depletion is linked to higher dust to gas ratios, at least in carbon rich PNe.

On the other hand errors in the derived iron gaseous abundances and consequently in the depletion factors are still too large to call for a really significantly higher depletion in NGC 7027 with respect to other (low reddening) nebulae as Hu 2-1 and Cn 3-1, in our sample.

It appears then worthwhile to pursue the point, by closely examining the iron behaviour particularly in other PNe having extreme reddening.

## References

- Acker A., Ochsenbein F., Stenholm B., et al., 1992, *Strasbourg-ESO Catalogue Of Galactic Planetary Nebulae*
- Aller L.H., Czyzak S.J., 1979, *Ap&SS* 62, 397
- Aller L.H., Czyzak S.J., 1983, *ApJS* 51, 211
- Anders E., Grevesse N., 1989, *Geochim. Cosmochim. Acta* 53, 197
- Barker T., 1978, *ApJ* 219, 914
- Beintema D.A., van Hoof P.A.M., Lohuis F., et al., 1996, *A&A* 315, L253
- Blocker T., 1995, *A&A* 299, 755
- Clegg R.E.S., Peimbert M., Torres-Peimbert S., 1987a, *MNRAS* 224, 761
- Clegg R.E.S., Harrington J.P., Barlow M.J., Walsh J.R., 1987b, *ApJ* 314, 551
- Cahn J.H., Kaler J.B., Stanghellini L., 1992, *A&AS* 94, 399
- Ferland G.J., 1996, *'Hazy, a brief introduction to Cloudy'*, University of Kentucky, Department of Physics and Astronomy, Internal Report
- French H.B., 1981, *ApJ* 246, 434
- Garstang R.H., 1962, *MNRAS* 124, 321
- Garstang R.H., Robb W.D., Rountree S.P., 1978, *ApJ* 222, 384
- Grevesse N., Noels, A., 1993, in "Origin of the Elements", eds. N. Prantzos, E. Vangioni-Flam, M. Casse', p.15 (Cambridge Univ. Press)
- Gurzadyan G.A., 1997, in "The Physics and Dynamics of Planetary Nebulae", Springer-Verlag, p. 119
- Henry R.B.C., Kwitter K.B., Howard J.W., 1996, *ApJ* 458, 215
- Hummer D.G., Storey P.J., 1987, *MNRAS* 224, 801
- Hummer D.G., Berrington K.A., Eissner W., et al., 1993, *A&A* 279, 298
- Kaler J.B., Jacoby G.H., 1991, *ApJ* 372, 215
- Keenan F.P., Norrington P.H., 1987, *A&A* 181, 370
- Keyes C.D., Aller L.H., Feibelman W.A., 1990, *PASP* 102, 59
- Kingsburgh R.L., English J., 1992, *MNRAS* 259, 635
- Lucy L.B., 1995, *A&A* 294, 555
- Mathis J.S., 1990, *ARA&A* 28, 37
- Middlemass D., 1990, *MNRAS* 244, 294
- Middlemass D., Clegg R.E.S., Walsh J.R., 1989, *MNRAS* 239, 1
- Miranda L.F., 1995, *A&A* 304, 531
- Miranda L.F., Vázquez R., Torrelles J.M., Eiroa C., López J.A., 1997, *MNRAS* 288, 777
- Nahar S.N., Pradhan A.K., 1996, *A&AS* 119, 509
- Nussbaumer H., Storey P.J., 1978, *A&A* 70, 37
- Nussbaumer H., Storey P.J., 1982, *A&A* 113, 21
- Nussbaumer H., Storey P.J., 1988, *A&A* 193, 327
- Paw T.H., Mo J.E., Pottasch S.R., 1984, *A&A* 139, L1
- Perinotto M., Panagia N., Benvenuti, P., 1980, *A&A* 85, 332
- Quinet P., 1996, *A&AS* 116, 573
- Quinet P., Le Dourneuf M. e Zeppen C.J., 1996, *A&AS* 120, 361
- Savage, B.D., Sembach, K.R., 1996, *ARA&A* 34, 279
- Shields G.A., 1975, *ApJ* 195, 475
- Shields G.A., 1978, *ApJ* 219, 559
- Zhang C.Y., Kwok S., 1993, *ApJS* 88, 137
- Zhang H.L., Pradhan A.K., 1995, *A&A* 293, 953
- Zhang H.L., 1996, *A&AS* 119, 523